Clonal Architecture and Evolutionary History of Waldenström's Macroglobulinemia at the Single-Cell Level

Ramón García-Sanz[1], María García-Álvarez[1,*], Alejandro Medina[1], Elham Askari[2], Verónica González-Calle[1], María Casanova[3], Igor de la Torre-Loizaga[1], Fernando Escalante-Barrigón[4], Miguel Bastos-Boente[1], Abelardo Bárez[5], Nerea Vidaña-Bedera[1], José María Alonso[6], María Eugenia Sarasquete[1], Marcos González[1], María Carmen Chillón[1], Miguel Alcoceba[1], and Cristina Jiménez[1]

1. Hematology Department, University Hospital of Salamanca (HUS/IBSAL), CIBERONC and Cancer Research Institute of Salamanca-IBMCC (USAL-CSIC), Salamanca, 37007, Spain
2. Hematology Department, Fundación Jiménez Díaz, Centro de Investigación Biomédica en Red-Cáncer, Madrid, 28040, Spain
3. Hematology Department, Hospital Costa del Sol, Marbella, 29603, Spain
4. Hematology Department, Complejo Asistencial Universitario de León, León, 24071, Spain
5. Hematology Department, Complejo Asistencial de Ávila, Ávila, 05071, Spain
6. Hematology Department, Complejo Asistencial Universitario de Palencia, Palencia, 34005, Spain

***Corresponding author:** María García-Álvarez
Email: mgarca1991@gmail.com
Hematology Department, University Hospital of Salamanca, Paseo de la Transición Española, 37007 Salamanca, Spain
Phone: +34 923 291100 Ext 56610

Key words: Disease mechanisms, Genomic alterations, Protein expression, Single-cell, Waldenström's macroglobulinemia

Summary statement

Our study shows for the first time the clonal architecture of Waldenström's macroglobulinemia at the single cell level, providing insight into how the oncogenic process can occur.

Abstract

To provide insight into the subclonal architecture and codependency patterns of the alterations in Waldenström's macroglobulinemia (WM), we performed single-cell

mutational and protein profiling of eight patients. A custom panel was designed to screen for mutations and copy number alterations at the single-cell level in samples taken from patients at diagnosis (n=5) or at disease progression (n=3). Results showed that in asymptomatic WM at diagnosis, *MYD88*^{L265P} was the predominant clonal alteration, while other events, if present, were secondary and subclonal to *MYD88*^{L265P}. In symptomatic WM, clonal diversity was more evident, uncovering combinations of alterations that synergized to promote clonal expansion and dominance. At disease progression, a dominant clone was observed, sometimes accompanied by other less complex minor clones, which could be consistent with a clonal selection process. Clonal diversity was also reduced, probably due to the effect of treatment. Finally, we combined protein expression with mutational analysis to map somatic genotype with the immunophenotype. Our findings provide a comprehensive view of the clonality of tumor populations in WM and how clonal complexity can evolve and impact disease progression.

INTRODUCTION

Waldenström's Macroglobulinemia (WM) is a distinct, indolent, B-cell lymphoproliferative disorder characterized by bone marrow infiltration by lymphoplasmacytic lymphoma and the presence of an immunoglobulin M (IgM) monoclonal component (Dogliotti et al., 2023; Owen et al., 2003). The cellular composition of this IgM lymphoma is variable, including malignant small lymphocytes, plasmacytoid lymphocytes, and plasma cells in variable percentages (Stone & Pascual, 2010). At the clinical level, the disease is consistently heterogeneous, with a behavior ranging from indolent forms, such as IgM monoclonal gammopathy of undetermined significance (IgM-MGUS) and asymptomatic WM, to highly symptomatic disease (symptomatic WM), with evolution being highly variable as well (Oza & Rajkumar, 2015).

Over the past decade, much progress has been made in the molecular understanding of WM through next generation sequencing large-scale bulk analyses. Genomic characterization of WM tumor cells has identified recurrent somatic mutations in *MYD88* (>95% patients) and *CXCR4* (>30% patients) genes, and deletions involving chromosome 6q (del6q, ~50% patients), among other alterations (Hunter et al., 2014; Schop et al., 2002; Treon et al., 2012). *MYD88*^{L265P} mutation is considered to be the tumor-initiating event that provides an advantage for B-cell clonal selection and predisposes the malignant clone to further genetic alterations, leading to full-blown lymphoma development (Alcoceba et al., 2022; Argyropoulos et al., 2016; Sewastianik

et al., 2019). However, most alterations are present in both symptomatic and asymptomatic WM, so the global genomic profile cannot explain the differences in the clinical behavior and evolution of the disease (Jiménez et al., 2018; Varettoni et al., 2017). The cell-of-origin of WM, the order of the events, their distribution in individual tumor cells and clones, and how these interact may be of great relevance to the course of the oncogenic process. However, by bulk sequencing it is not possible to obtain that information, because cell identities are not preserved. Innovative single-cell sequencing technologies allow to dissect the tumor genetic heterogeneity and accurately measure clonal complexity, deciphering the patterns of somatic mutations across clonal populations (García‐sanz & Jiménez, 2021). As tumors are constantly evolving, they often contain mutations that are relatively rare when they first emerge. Detecting these mutations and the clones that carry them may be of clinical importance for minimal residual disease, therapeutic resistance or disease progression and transformation (Demaree et al., 2021; Guess et al., 2022; Meyers et al., 2022; Nadeu et al., 2022; Robinson et al., 2022; Wang et al., 2022).

To date, there are few studies of WM at the single-cell level (Cholujova et al., 2023; Kaushal et al., 2021; Mondello et al., 2023; Rodriguez et al., 2022; Sun et al., 2022). Only one of these studies is based on DNA-sequencing, and although it allowed to identify the presence of *MYD88*^{L265P} in B-cell precursors, it did not provide data on the order of mutation acquisition, co-mutation patterns, or how the mutational landscape fluctuates over the course of the disease (Rodriguez et al., 2022). We have performed an integrated single-cell DNA sequencing and immunophenotyping study to establish the sequence of genetic events, the target populations in which they arise, and the co-dependency/exclusion of alterations. We have analyzed the cell populations at baseline and following therapy to better understand the tumor architecture and evolutionary trajectories underlying the oncogenic process. The correlation with the immunophenotype provided information about the different cell populations present and whether they were part of the neoplastic clone.

RESULTS

A total of 42,352 cells were used for single-cell analysis (median 3839 cells/patient; range, 1031–11307 cells). Patients' medical history and immunophenotype of the samples used (marked in bold) are described in Table 1.

Tumor architecture & order of the events

First, analysis showed that *MYD88*^{L265P} was the most clonal alteration at diagnosis. MW1 and MW2 were both diagnostic samples of asymptomatic WM. *MYD88* mutation defined the main tumor clone in these patients (it was present in 91.5% and 26.5% of cells, respectively). Part of the clone (~25% and ~16% of cells, respectively) had acquired del6q, confirming that it was a secondary alteration that appears after *MYD88* mutation (Fig. 1A-B). In MW3 and MW4 (both symptomatic WM at diagnosis), *MYD88*^{L265P} was also clonal (80.4% and 89.7% of cells, respectively), but no further alterations were detected. MW5 was diagnosed as IgM-MGUS (in 2017), and four years later progressed to symptomatic WM. We analyzed the sample of progression to symptomatic WM. At that time, two subclones could be differentiated: *MYD88*-del6q-del17p-amp3q (12.2%, colored in blue in Fig. 1C), and *MYD88*-del6q-*CXCR4* (1.2%, in yellow). Both had in common *MYD88*^{L265P} and del6q, but then one of the subclones acquired a *CXCR4* mutation, while the other one acquired del17p and amp3q. A branching model of disease evolution can be inferred based on this clonal distribution (Fig. 1C).

In samples taken at the time of disease progression, the scenario changed. The secondary alterations were (mostly) present in the same cells as *MYD88*^{L265P}. MW6 was a symptomatic WM, and we analyzed the sample of progression after the second line of treatment. The main tumor clone of this patient (56.8% of cells) presented *CXCR4* mutation and was homozygous for *MYD88*^{L265P} possibly due to an acquired uniparental disomy (aUPD) of chr3. Interestingly, there were two additional small subclones without the loss of the chr3 copy: one with the *MYD88* mutation only (0.6%), and the second one with both *MYD88* and *CXCR4* mutations (2.5%) (Fig. 1D). These two small clones could represent the initial clones, which shed light on how the oncogenic process may have occurred. MW7 was first diagnosed as IgM-MGUS, and 10 years later progressed to symptomatic WM. The sample analyzed was the progression after the first line of treatment. The alterations this patient had (del6q and amp3q) co-occurred in the same cells as *MYD88* mutation, and in this case, there were no remaining cells representing any potential ancestor (Fig. 1E). Finally, MW8 was a patient diagnosed as asymptomatic WM, who progressed to symptomatic WM. The sample included corresponded to the time of progression after ibrutinib therapy (second line). This sample had a del6q that, according to FISH results, was not present in the samples at diagnosis or when the patient progressed to symptomatic WM. The subclone having this alteration (~6.6% of the CD19+ cells), along with del*TRAF3*, may

therefore be considered emergent at the time of ibrutinib progression (Fig. 1F). Predicted evolution of the events based on these observations is presented in Fig. S1).

Co-occurrence & exclusion of alterations

Next, we investigated the co-dependency and exclusion of alterations at single-cell resolution. As we have just mentioned, we detected *MYD88*^{L265P} variant in all patients (8/8), defining the main clone and supporting its role as the tumor-initiating event. Secondary oncogenic events, such as del6q (present in 5/8 patients), *CXCR4* mutations (2/8 patients), amp3q (2/8 patients), del*TRAF3* (1/8 patients), and del17p (1/8 patients), accompanied *MYD88* mutation. *CXCR4* mutations were subclonal to *MYD88* at diagnosis (MW5, Fig. 1C), but not at disease progression (MW6, Fig. 1D), as it happened with amp3q (MW5, Fig. 1C, and MW7, Fig. 1E, respectively). Del6q was subclonal to *MYD88* at diagnosis in asymptomatic WM (MW1 and MW2, Fig. 1A,B) but not in symptomatic WM (MW5, Fig. 1C). Finally, the aUPD of chr3 co-ocurred with *CXCR4* mutation (MW6, Fig. 1D).

We also observed that alterations with a common role could concur in the same cells. Thus, deletions of two negative regulators of the NF-κB signaling pathway, *TRAF3* and *TNFAIP3* (i.e., del6q), co-occurred in the same subclone in one patient (MW8, Fig. 1F). Del6q (*TNFAIP3*) also coexisted with amp3q, which includes *TBL1XR1*, a gene involved in the activation of NF-κB, in two patients (MW5, Fig. 1C, and MW7, Fig. 1E). On the contrary, del6q always showed mutual exclusivity with *CXCR4* mutations, except in a minority subclone of one patient, suggesting they are two different pathways that can promote disease progression. In the majority clone of this patient, del6q co-occurred with del17p and amp3q (MW5, Fig. 1C). However, all findings are based on very few numbers and therefore must be interpreted with caution.

MYD88^{L265P} *in normal B cells*

MYD88 mutation has been recently found in immunophenotypically normal B cells of WM patients (Kaushal et al., 2021; Rodriguez et al., 2022). To confirm these findings, we compared the percentage of clonal B cells by FCM, defined by the monoclonal light chain restriction, with the percentage of cells having *MYD88* mutation. For results to be comparable, we calculated the percentage of tumor cells out of the total mononuclear cells (in patients MW2, MW5, MW6 & MW7), and out of the total CD19+ cells in samples with CD19 negative depletion (i.e., MW1, MW3, MW4 & MW8). Overall, numbers were similar, but patients MW2, MW3 & MW6 presented a higher percentage

of *MYD88*-mutated cells (26.5%, 80.4%, and 59.9%, respectively) than clonal cells (B lymphocytes and plasma cells) by FCM (20.4%, 63%, and 45.2%, respectively), which concurs with the existence of *MYD88*-mutated non-clonal cells.

Single-cell protein sequencing analysis

Protein analysis was based on the expression of CD34, CD19, CD20 and CD38 antigens. Protein libraries of patients MW2 and MW4 failed (so no expression data were available for these cases), and CD19 antibody did not work in MW7. According to FCM data, immature cells (named B-cell precursors) were defined as CD34+CD19+CD20-CD38+, B lymphocytes as CD34-CD19+CD20+CD38-, and plasma cells/plasmacytoid lymphocytes as CD34-CD19+CD20+CD38+. Cells with a phenotype not consistent with any of the above were removed from the final plots. Clonality of B cells could not be assessed based on these markers.

Despite these difficulties, analysis showed that alterations were present in all cell populations, and likewise, all populations had wild-type cells (at least for the alterations evaluated with this panel) (Fig. S2A,C). In addition, slight phenotypic differences could be observed in mutated vs. wild-type cells within each population (Fig. S2A) and in all cells in patients in whom CD19-selection was not performed (Fig. S2B): MW5 (CD19 and CD38 expression), MW6 (CD19, CD38 and CD34 expression), and MW7 (CD20 and CD38 expression). Thus, mutated cells expressed CD19 or CD20 more strongly, while CD34 and CD38 expression was weaker than in unmutated cells (Fig. S2B). In samples with depletion of CD19 negative cells (MW1, MW3 and MW8), these differences could not be so well appreciated because most cells were *MYD88*-mutated (Fig. S2C-D). In MW1, when we clustered the cells based on protein expression, we could observe that the 6q region studied (genes *IBTK*, *PRDM1*, *BCLAF1* and *TNFAIP3*) was not completely and equally deleted in all cells, appearing that *TNFAIP3* was the first gene to be deleted, and the most common in the immature cells (Fig. 2).

DISCUSSION

The genomic landscape of WM has been well described, and allowed to characterize disease mechanisms and to identify biomarkers and therapeutic targets (Braggio et al., 2009; Hunter et al., 2014; Jiménez et al., 2018; Poulain et al., 2013; Schop et al., 2002; Treon et al., 2012; Varettoni et al., 2017). By bulk sequencing, it is possible to infer patterns of clonality, sub-clonality and clonal evolution using VAF distribution. However,

single-cell techniques can provide more detailed and direct approaches to study intratumor heterogeneity and clonal architecture. Here we have performed a single-cell DNA and protein sequencing study in WM with the Tapestri platform. Single-cell analysis assigns alterations to different clones allowing to reconstruct tumor evolutionary histories and to identify disease-initiating events, as well as cooperative mutations that give cells a fitness advantage (Navin et al., 2011).

Genetic evidence supports a stepwise accumulation of genomic alterations (mutations, copy-number abnormalities, loss of heterozygosity) during WM development, suggesting they have a role in the multistep oncogenic process that drives this transition (Jiménez et al., 2018; Paiva et al., 2015; Poulain et al., 2013; Varettoni et al., 2017). Thus, we found that clonal complexity increased as disease evolved, but that could also be reduced due to the effect of treatment. The presence of more mature subclonal populations with higher number of genetic alterations (*MYD88*, *CXCR4*, del6q, del17p, amp3q) was associated with more advanced and symptomatic disease that required treatment. Considering the distribution of the alterations within the different subclones and their respective clonality, we proved that *MYD88*^{L265P} was the common driver event, and that only clones containing *MYD88* mutation gave rise to more aggressive populations by acquiring new alterations. Depending on the clone in which they arise, these alterations may give certain cells a fitness advantage, resulting in the intraclonal heterogeneity seen in WM and the different models of tumor evolution (Bolli et al., 2014; Greaves & Maley, 2012). Patient MW5 could represent an example of branched evolution, as two separated subclones (one with del17p and amp3q, and the other with *CXCR4* mutation) derived from a common ancestor that harbored *MYD88*^{L265P} and del6q. The expansion of both clones is restrained by a mutual competition known as clonal interference (Anderson et al., 2011).

Previous studies point that there might be at least two distinct oncogenic pathways that promote progression to symptomatic disease in WM: mutated *CXCR4* and del6q (Cao et al., 2015; Guerrera et al., 2018; Hunter et al., 2016; Roccaro et al., 2014). Loss of chromosome 6q is found in 40-50% of patients with WM and appears exclusive of *CXCR4* in treatment-naïve patients, suggesting shared roles for the two genomic events (Guerrera et al., 2018; Schop et al., 2002). We found del6q in 5/8 patients, showing mutual exclusivity with *CXCR4* mutations in all but one patient (MW5), and even in this case, the subclone in which both alterations co-occurred was minority. The predominant subclone of this patient had del6q, amp3q and del17p, suggesting these are cooperative alterations that provide cells a proliferative advantage. We also found other alterations that induce the same mechanism, such as del6q and del*TRAF3*, or

del6q and amp3q, all of them leading to the activation of the NF-κB signaling pathway, coexisting in the same patients, and even in the same subclones (Braggio et al., 2009; Jung et al., 2017).

The changes in the tumor architecture observed at disease progression could be attributed to a cancer-clone evolutionary selection for more robust or malignant phenotypes (Greaves & Maley, 2012). In patient MW6, the few remaining cells having less alterations (*MYD88*^{L265P} alone or *MYD88*^{L265P} plus *CXCR4* mutation) than the main clone could represent the initial clones, illustrating how the oncogenic process may have occurred: *MYD88*^{L265P} was the initial oncogenic event, then *CXCR4* mutation was acquired and finally, the aUPD of chr3, both being present in the same subclone. The aUPD may have potentially contributed to clonal evolution by rendering tumor cells homozygous for a pre-existing oncogenic mutation (*MYD88*^{L265P}) (Treon et al., 2016). In MW7 the scenario was similar, but since no remnants of the potential initial clones could be observed, the temporal ordering of genomic events could not be inferred. Both functionally relevant mutational events and therapy can drive clonal selection, but to gain more detailed insight into clonal trajectories in individual patients, this issue needs to be best addressed by serial sampling (Bolli et al., 2014; Greaves & Maley, 2012). Our last case (MW8) may exemplify the emergence of *new* clones resistant to therapy. Del6q has been associated to disease progression (García-Sanz et al., 2021) and ibrutinib resistance in WM (Jimenez et al., 2020). Since this alteration was not present in the previous moments (according to FISH), it could be hypothesized that the subclone with del6q and del*TRAF3* is responsible for the treatment resistance acquisition, especially considering that the patient did not have mutations in *BTK* (Xu et al., 2017). However, considering that the sensitivity of FISH does not reach the single-cell level, we also cannot discard the possibility that new selective pressures (i.e., ibrutinib therapy) had allowed pre-existing cancer cells that survived treatment to emerge. Alterations in *CXCR4*, have also been reported as associated with drug resistance, including resistance to Ibrutinib (Cao et al., 2015; Roccaro et al., 2014; Treon et al., 2015). In our series, only two patients harbored these alterations but did not show treatment resistance.

Single-cell techniques allow not only to establish the events order, but also the sequence of acquisition of structural variants. In the asymptomatic WM (MW1), among the genes we evaluated, *TNFAIP3* seemed to be the most frequently deleted gene, which suggests that del6q may begin to happen around this area. In symptomatic WM, the entire 6q region evaluated was equally deleted.

Contrary to other works (Rodriguez et al., 2022), we did not find wild-type *MYD88* in tumor cells carrying other genetic lesions, at least for the alterations we studied. However, based on the comparison of the tumor infiltration by flow cytometry and the percentage of cells carrying *MYD88* mutation by single-cell analysis, we were able to confirm that this alteration can be present in phenotypically normal B cells of WM patients (Rodriguez et al., 2022). Emerging evidence has suggested that *MYD88*^{L265P} would arise during hematopoietic development, although not always at the same cellular stage, and that parallel clonal expansions occur before subclones begin to dominate in early cancer development but are rare after cell transformation (Anderson et al., 2011; Rodriguez et al., 2022; Siegmund et al., 2009). Most somatic mutations present in progenitor cells are undetectable in mature B lymphocytes, suggesting continuous clonal selection until oncogenic alterations appear and cause the transformation. We have observed slight differences in the immunophenotype of *MYD88*-mutated compared to wild-type cells. Therefore, one might think that the acquisition of *MYD88* mutation would be accompanied by changes in the immunophenotype as the B-cell clone progressively grows and evolves. The immune microenvironment has been shown to play a critical role in this transition (Kaushal et al., 2021).

Single-cell data may have biological and therapeutic relevance in the future. Intratumor heterogeneity has been shown to be prognostic in certain cancer types and can also explain the partial efficacy of targeted therapies (Andor et al., 2016; Landau et al., 2013; Rocco, 2015; Yates et al., 2015) or why it is impossible to achieve complete responses with BTK inhibitors as monotherapy in WM (Buske et al., 2022; Tam et al., 2020). Current treatment approaches typically consider the disease to be static and homogeneous. Understanding the heterogeneity within tumors and their ability to evolve in response to therapy may allow to design interventions to disrupt clonal evolution and/or target WM as a multi-clonal disease. Also, the identification of subclones potentially associated with treatment resistance may allow the use of preventive therapeutic strategies.

We are aware of the limitations of our study, especially the number of patients, not having sequential samples, the gene panel size, and the use of a new methodology. Nevertheless, our results are supported by FISH and flow cytometry studies.

In summary, we have precisely characterized the clonal architecture of WM at the single-cell level for the first time. Our work including the different stages of WM (asymptomatic, symptomatic, and symptomatic post-therapy) provides information

about how disease initiates and progresses, the timing of the alterations (early vs. late), the cooperative mutations, and the patterns of evolution.

MATERIALS AND METHODS

Patients and samples

Eight WM patients –five at diagnosis and three at the time of disease progression– were included in the study. Cases were diagnosed using standard WHO classification criteria (2016 update) (Swerdlow et al., 2016), which was fully concordant with the new updates (Alaggio et al., 2022; Campo et al., 2022). Samples were selected based on the tumor infiltration detected by flow cytometry (FCM) during the standard diagnostic process. Mononuclear cells were isolated from bone marrow by Ficoll-Paque density-gradient centrifugation, and CD19 negative cells were removed with the EasySep™ Human B Cell Enrichment Kit (STEMCELL Technologies, Inc.) when sufficient cells were available (patients MW1, MW3, MW4 and MW8). Cells were preserved in fetal bovine serum with 10% DMSO (dimethyl sulfoxide) at -80º until used for single-cell studies. Previous and/or subsequent samples from these patients were evaluated by FISH, flow cytometry and molecular studies to help understand the evolutionary history of the tumors. The study was approved by the ethics committee following the ethical recommendations and guidelines of the Declaration of Helsinki. Written informed consent was obtained from all eight patients.

Single-cell DNA and protein sequencing

We designed a Tapestri™ Single-Cell DNA Custom Panel of 112 amplicons (Mission Bio, San Francisco, CA) covering the hotspot regions of 20 genes (*MYD88*, *CXCR4*, *ARID1A*, *KMT2D*, *TP53*, *CD79A*, *CD79B*, *NOTCH2*, *TRAF2*, *TRAF3*, *MYBBP1A*, *HIST1H1E*, *KLF2*, *TBL1XR1*, *PTPN13*, *RAG2*, and *IBTK*, *PRDM1*, *BCLAF1* and *TNFAIP3*, for the assessment of 6q deletion), and an antibody-oligo conjugated panel targeting the following surface proteins: CD19, CD20, CD34, CD38, and CD138. CD34 oligo-conjugated antibody was used in a 1:2 dilution, CD38 in a 1:5 dilution, and the remaining antibodies were used without dilution. Due to its overexpression compared to the other proteins, CD138 was removed from the final analysis.

Simultaneous profiling of DNA mutation and cell-surface immunophenotype was performed according to the manufacturer's protocol. Cell suspensions had to contain

6,000-10,000 cells/µl at ≥80% viability to be processed. Briefly, cryopreserved bone marrow mononuclear cells were thawed, quantified, and stained with the pool of 5 oligo-conjugated antibodies. The stained cells were washed and loaded into the Tapestri instrument for single-cell encapsulation, lysis, and barcoding. Targeted amplification using multiplexed PCR occurred within the droplets. DNA and protein PCR products were then isolated from the individual droplets, purified with AMPure XP beads (Beckman Coulter, Inc.) and streptavidin beads (Thermo Fisher Scientific, Inc.), and used for library generation. DNA and antibody-tagged final libraries were quantified using Qubit 4 fluorometer (Thermo Fisher Scientific, Inc.) and pooled for sequencing on a NextSeq 1000/2000 sequencer (Illumina, San Diego, CA) using 2x150 bp cycles.

Data analysis

Raw FASTQ files were processed with the Tapestri pipeline v2 (Mission Bio), which includes adapter-trimming using Cutadapt, alignment to the reference human genome GRCh37/hg19 using Burrows-Wheeler Aligner, cellular barcode demultiplexing, and cell-based genotype calling using GATK/HaplotypeCaller. The output .loom files were analyzed using Tapestri Insights (v2.2), filtering out low-quality genotypes and cells (i.e., genotype quality <30, reads/cell/target <10, mutant variant allele frequency (VAF) <20%, variants mutated in <1% of the cells, and cells with <50% of genotypes present). The python-based Mosaic analysis package (https://github.com/MissionBio/mosaic) was used for more advanced multiomics analysis and data visualization of the .h5 files. Only cells with complete genotype information of the variants selected for downstream analysis were included.

Flow cytometry immunophenotyping

Bone marrow samples were processed following the general recommendations of the EuroFlow group (Kalina et al., 2012) and stained with at least an 8-color panel including the following monoclonal antibodies combined in several tubes: surface immunoglobulin-M (SIgM), CD5, CD19, CD20, CD22, CD23, CD25, CD27, CD38, CD45, CD56, CD79b, CD81, CD117, CD138, and intracytoplasmic IgM (CyIgM), kappa (CyK) and lambda (Cyλ). A minimum of 1 million cells were acquired per tube in a FACSCalibur flow cytometer (Becton Dickinson Biosciences, San Jose, CA) using BD FACSDiva™ software v6.1. Data were analyzed using Infinicyt™ software v2.0 (Cytognos, Salamanca, Spain). Light chain-restricted clonal lymphocytes (CD19+) and

plasma cells (CD38+ or strong CD138+) were quantified (Paiva et al., 2014; Puig et al., 2017).

FISH studies

Simple interphase fluorescence in situ hybridization (FISH) was performed on cell nuclei of CD19+ cells from bone marrow samples using our previously published techniques (Ocio et al., 2005). Deletions of 6q and 17p, and translocations of 14q32 were evaluated. At least 100 cells were analyzed in all samples, applying Vysis scoring criteria (Abbott Laboratories, Abbott Park, IL). The cutoff point for the identification of an alteration was set at ≥10% cells with an abnormal signal.

Acknowledgements

The authors thank José Juan Pérez, Alicia Antón, Rebeca Maldonado, Ana Balanzategui, Estrella Arnés, Ana Isabel Sánchez, Montserrat Hernández, Mª Inmaculada Sánchez and Sandra María Lucas for their technical assistance.

Competing interests

No competing interests declared.

Funding

This work was supported by Instituto de Salud Carlos III through the projects PI18/01866 (Co-funded by European Regional Development Fund “A way to make Europe”) and PI21/00568 (Co-funded by the European Union). C.J. was supported by Instituto de Salud Carlos III (Contrato Sara Borrell CD19/00030).

Author contributions

Conceptualization and designing: R.G.S., C.J.; Methodology and investigation: R.G.S., M.G.A., M.A., C.J.; Providing patients and clinical data: R.G.S., E.A., V.G.C., M.C., F.E.B., A.B., J.M.A., M.G.; Analysis and results interpretation: M.G.A., A.M., I.T.L., M.B.B., N.V.B., M.E.S., M.C.C., M.A., C.J.; Writing—original draft preparation: C.J.; Writing—review and editing: R.G.S.; Funding acquisition: R.G.S., C.J.

References

Alaggio, R., Amador, C., Anagnostopoulos, I., Attygalle, A. D., Araujo, I. B. de O., Berti, E., Bhagat, G., Borges, A. M., Boyer, D., Calaminici, M., Chadburn, A., Chan, J. K. C., Cheuk, W., Chng, W.-J., Choi, J. K., Chuang, S.-S., Coupland, S. E., Czader, M., Dave, S. S., … Xiao, W. (2022). The 5th edition of the World Health Organization Classification of Haematolymphoid Tumours: Lymphoid Neoplasms. *Leukemia*, *36*(7), 1720–1748. https://doi.org/10.1038/s41375-022-01620-2

Alcoceba, M., García-álvarez, M., Medina, A., Maldonado, R., González-Calle, V., Chillón, M. C., Sarasquete, M. E., González, M., García-Sanz, R., & Jiménez, C. (2022). MYD88 Mutations: Transforming the Landscape of IgM Monoclonal Gammopathies. *International Journal of Molecular Sciences*, *23*(10), 5570. https://doi.org/10.3390/ijms23105570

Anderson, K., Lutz, C., Van Delft, F. W., Bateman, C. M., Guo, Y., Colman, S. M., Kempski, H., Moorman, A. V., Titley, I., Swansbury, J., Kearney, L., Enver, T., & Greaves, M. (2011). Genetic variegation of clonal architecture and propagating cells in leukaemia. *Nature*, *469*(7330), 356–361. https://doi.org/10.1038/nature09650

Andor, N., Graham, T. A., Jansen, M., Xia, L. C., Aktipis, C. A., Petritsch, C., Ji, H. P., & Maley, C. C. (2016). Pan-cancer analysis of the extent and consequences of intratumor heterogeneity. *Nature Medicine*, *22*(1), 105–113. https://doi.org/10.1038/nm.3984

Argyropoulos, K., Vogel, R., Ziegler, C., Altan-Bonnet, G., Velardi, E., Calafiore, M., Dogan, A., Arcila, M., Patel, M., Knapp, K., Mallek, C., & Hunter, Z. (2016). Clonal B cells in Waldenström's macroglobulinemia exhibit functional features of chronic active B-cell receptor signaling. *Leukemia*, *30*(108), 1116–1125. https://doi.org/10.1038/leu.2016.8

Bolli, N., Avet-Loiseau, H., Wedge, D. C., Van Loo, P., Alexandrov, L. B., Martincorena, I., Dawson, K. J., Iorio, F., Nik-Zainal, S., Bignell, G. R., Hinton, J. W., Li, Y., Tubio, J. M. C., McLaren, S., O' Meara, S., Butler, A. P., Teague, J. W., Mudie, L., Anderson, E., … Munshi, N. C. (2014). Heterogeneity of genomic evolution and mutational profiles in multiple myeloma. *Nature Communications*, *5*, 2997. https://doi.org/10.1038/ncomms3997

Braggio, E., Keats, J. J., Leleu, X., Van Wier, S., Jimenez-Zepeda, V. H., Valdez, R., Schop, R. F. J., Price-Troska, T., Henderson, K., Sacco, A., Azab, F., Greipp, P., Gertz, M., Hayman, S., Rajkumar, S. V., Carpten, J., Chesi, M., Barrett, M., Stewart, A. K., … Fonseca, R. (2009). Identification of copy number abnormalities and inactivating mutations in two negative regulators of nuclear factor-kB signaling pathways in Waldenström's macroglobulinemia. *Cancer Research*, *69*(8), 3579–3588. https://doi.org/10.1158/0008-5472.CAN-08-3701

Buske, C., Tedeschi, A., Trotman, J., García-Sanz, R., MacDonald, D., Leblond, V., Mahe, B., Herbaux, C., Matous, J. V., Tam, C. S., Heffner, L. T., Varettoni, M., Palomba, M. L., Shustik, C., Kastritis, E., Treon, S. P., Ping, J., Hauns, B., Arango-Hisijara, I., & Dimopoulos, M. A. (2022). Ibrutinib Plus Rituximab Versus Placebo Plus Rituximab for Waldenström's Macroglobulinemia: Final Analysis From the Randomized Phase III iNNOVATE Study. *Journal of Clinical Oncology*, *40*(1), 52–62. https://doi.org/10.1200/jco.21.00838

Campo, E., Jaffe, E. S., Cook, J. R., Quintanilla-Martinez, L., Swerdlow, S. H., Anderson, K. C., Brousset, P., Cerroni, L., de Leval, L., Dirnhofer, S., Dogan, A., Feldman, A., Fend, F., Friedberg, J. W., Gaulard, P., Ghia, P., Horwitz, S. M., King, R. L., Salles, G. A., … Zelenetz, A. D. (2022). The International Consensus Classification of Mature Lymphoid Neoplasms: A Report from the Clinical Advisory Committee. *Blood*, *140*(11), 1229–1253. https://doi.org/10.1182/blood.2022015851

Cao, Y., Hunter, Z. R., Liu, X., Xu, L., Yang, G., Chen, J., Patterson, C. J., Tsakmaklis, N., Kanan, S., Rodig, S., Castillo, J. J., & Treon, S. P. (2015). The WHIM-like CXCR4 S338X somatic mutation activates AKT and ERK, and promotes resistance to ibrutinib and other agents used in the treatment of Waldenstrom's Macroglobulinemia. *Leukemia*, *29*(1), 169–176. https://doi.org/10.1038/leu.2014.187

Cholujova, D., Beke, G., Hunter, Z. R., Hideshima, T., Flores, L., Zeleznikova, T., Harrachova, D., Klucar, L., Leiba, M., Drgona, L., Treon, S. P., Kastritis, E., Dorfman, D. M., Anderson, K. C., & Jakubikova, J. (2023). Dysfunctions of innate and adaptive immune tumor microenvironment in Waldenström macroglobulinemia. *International Journal of Cancer*, *152*(9), 1947–1963. https://doi.org/10.1002/ijc.34405

Demaree, B., Delley, C. L., Vasudevan, H. N., Peretz, C. A. C., Ruff, D., Smith, C. C., & Abate, A. R. (2021). Joint profiling of DNA and proteins in single cells to dissect genotype-phenotype associations in leukemia. *Nature Communications*, *12*(1), 1–10. https://doi.org/10.1038/s41467-021-21810-3

Dogliotti, I., Jiménez, C., Perez, J. J., Morel, P., Varettoni, M., Talaulikar, D., Bagratuni, T., Ferrante, M., Pérez, J., Drandi, D., Puig, N., Gilestro, M., García-Álvarez, M., Owen, R., Jurczak, W., Tedeschi, A., Leblond, V., Kastritis, E., Kersten, M. J., … García-Sanz, R. (2023). Diagnostics in Waldenström's macroglobulinemia: a consensus statement of the European Consortium for Waldenström's Macroglobulinemia. *Leukemia*, *37*(2), 388–395. https://doi.org/10.1038/S41375-022-01762-3

García-Sanz, R., Dogliotti, I., Zaccaria, G. M., Ocio, E. M., Rubio, A., Murillo, I., Escalante, F., Aguilera, C., García-Mateo, A., García de Coca, A., Hernández, R., Dávila, J., Puig, N., García-Álvarez, M., Chillón, M. del C., Alcoceba, M., Medina, A., González de la Calle, V., Sarasquete, M. E., … Jiménez, C. (2021). 6q deletion in Waldenström macroglobulinaemia negatively affects time to transformation and survival. *British Journal of Haematology*, *192*(5), 843–852. https://doi.org/10.1111/bjh.17028

García-sanz, R., & Jiménez, C. (2021). Time to move to the single-cell level: Applications of single-cell multi-omics to hematological malignancies and waldenström's macroglobulinemia—a particularly heterogeneous lymphoma. *Cancers*, *13*(7), 1541. https://doi.org/10.3390/cancers13071541

Greaves, M., & Maley, C. C. (2012). Clonal evolution in cancer. *Nature*, *481*(7381), 306–313. https://doi.org/10.1038/nature10762

Guerrera, M. L., Tsakmaklis, N., Xu, L., Yang, G., Demos, M., Kofides, A., Chan, G. G., Manning, R. J., Liu, X., Chen, J. G., Munshi, M., Patterson, C. J., Castillo, J. J., Dubeau, T., Gustine, J., Carrasco, R. D., Arcaini, L., Varettoni, M., Cazzola, M., … Hunter, Z. R. (2018). MYD88 mutated and wild-type Waldenström's Macroglobulinemia: Characterization of chromosome 6q gene losses and their mutual exclusivity with mutations in CXCR4. *Haematologica*, *103*(9), e408–e411. https://doi.org/10.3324/haematol.2018.190181

Guess, T., Potts, C. R., Bhat, P., Cartailler, J. A., Brooks, A., Holt, C., Yenamandra, A., Wheeler, F. C., Savona, M. R., Cartailler, J.-P., & Ferrell, P. B. (2022). Distinct Patterns of Clonal Evolution Drive Myelodysplastic Syndrome Progression to Secondary Acute Myeloid Leukemia. *Blood Cancer Discovery*, *3*(4), 316–329. https://doi.org/10.1158/2643-3230.bcd-21-0128

Hunter, Z. R., Xu, L., Yang, G., Tsakmaklis, N., Vos, M., Liu, X., Chen, J. J. G., Manning, R. J., Chen, J. J. G., Patterson, C. J., Gustine, J., Debeau, T., Jorge, J., Anderson, K. C., Munshi, N. M., Treon, S. P., Vos, J. M., Liu, X., Chen, J. J. G., … Treon, S. P. (2016). Transcriptome sequencing reveals a profile that corresponds to genomic variants in Waldenström macroglobulinemia. *Blood*, *128*(6), 827–838. https://doi.org/10.1182/blood-2016-03-708263

Hunter, Z. R., Xu, L., Yang, G., Zhou, Y., Liu, X., Cao, Y., Manning, R. J., Tripsas, C., Patterson, C. J., Sheehy, P., & Treon, S. P. (2014). The genomic landscape of Waldenström macroglobulinemia is characterized by highly recurring MYD88 and WHIM-like CXCR4 mutations, and small somatic deletions associated with B-cell lymphomagenesis. *Blood*, *123*(11), 1637–1646. https://doi.org/10.1182/blood-2013-09-525808

Jimenez, C., Chan, G. G., Xu, L., Tsakmaklis, N., Kofides, A., Demos, M. G., Chen, J., Liu, X., Munshi, M., Yang, G., Wiestner, A., Garcia-sanz, R., Treon, S. P., Hunter, Z. R., Jiménez, C., Chan, G. G., Xu, L., Tsakmaklis, N., Kofides, A., … Hunter, Z. R. (2020). Genomic evolution of ibrutinib-resistant clones in Waldenström macroglobulinaemia. *British Journal of Haematology*, *189*(6), 1165–1170. https://doi.org/10.1111/bjh.16463

Jiménez, C., Prieto-Conde, M. I., García-Álvarez, M., Alcoceba, M., Escalante, F., Chillón, M. D. C., García de Coca, A., Balanzategui, A., Cantalapiedra, A., Aguilar, C., Corral, R., González-López, T., Marín, L. A., Bárez, A., Puig, N., García-Mateo, A., Gutiérrez, N. C., Sarasquete, M. E., González, M., & García-Sanz, R. (2018). Unraveling the heterogeneity of IgM monoclonal gammopathies: a gene mutational and gene expression study. *Annals of Hematology*, *97*(3), 475–484. https://doi.org/10.1007/s00277-017-3207-3

Jung, H., Yoo, H. Y., Lee, S. H., Shin, S., Kim, S. C., Lee, S., Joung, J.-G., Nam, J.-Y., Ryu, D., Yun, J. W., Choi, J. K., Ghosh, A., Kim, K. K., Kim, S. J., Kim, W. S., Park, W.-Y., & Ko, Y.-H. (2017). The mutational landscape of ocular marginal zone lymphoma identifies frequent alterations in TNFAIP3 followed by mutations in TBL1XR1 and CREBBP. *Oncotarget*, *8*(10), 17038–17049. https://doi.org/10.18632/oncotarget.14928

Kalina, T., Flores-Montero, J., Van Der Velden, V. H. J., Martin-Ayuso, M., Böttcher, S., Ritgen, M., Almeida, J., Lhermitte, L., Asnafi, V., Mendonça, A., De Tute, R., Cullen, M., Sedek, L., Vidriales, M. B., Pérez, J. J., Te Marvelde, J. G., Mejstrikova, E., Hrusak, O., Szczepaski, T., … Orfao, A. (2012). EuroFlow standardization of flow cytometer instrument settings and immunophenotyping protocols. *Leukemia*, *26*(9), 1986–2010. https://doi.org/10.1038/leu.2012.122

Kaushal, A., Nooka, A. K., Carr, A. R., Pendleton, K. E., Barwick, B. G., Manalo, J., McCachren, S. S., Gupta, V. A., Joseph, N. S., Hofmeister, C. C., Kaufman, J. L., Heffner, L. T., Ansell, S. M., Boise, L. H., Lonial, S., Dhodapkar, K. M., & Dhodapkar, M. V. (2021). Aberrant Extrafollicular B Cells, Immune Dysfunction, Myeloid Inflammation, and MyD88-Mutant Progenitors Precede Waldenstrom Macroglobulinemia. *Blood Cancer Discovery*, *2*(6), 600–615. https://doi.org/10.1158/2643-3230.bcd-21-0043

Landau, D. A., Carter, S. L., Stojanov, P., McKenna, A., Stevenson, K., Lawrence, M. S., Sougnez, C., Stewart, C., Sivachenko, A., Wang, L., Wan, Y., Zhang, W., Shukla, S. A., Vartanov, A., Fernandes, S. M., Saksena, G., Cibulskis, K., Tesar, B., Gabriel, S., … Wu, C. J. (2013). Evolution and impact of subclonal mutations in chronic lymphocytic leukemia. *Cell*, *152*(4), 714–726. https://doi.org/10.1016/j.cell.2013.01.019

Meyers, S., Alberti-Servera, L., Gielen, O., Erard, M., Swings, T., De Bie, J., Michaux, L., Dewaele, B., Boeckx, N., Uyttebroeck, A., De Keersmaecker, K., Maertens, J., Segers, H., Cools, J., & Demeyer, S. (2022). Monitoring of Leukemia Clones in B-cell Acute Lymphoblastic Leukemia at Diagnosis and during Treatment by Single-cell DNA Amplicon Sequencing. *HemaSphere*, *6*(4), E700. https://doi.org/10.1097/HS9.0000000000000700

Mondello, P., Paludo, J., Novak, J. P., Wenzl, K., Yang, Z.-Z., Jalali, S., Krull, J. E., Braggio, E., Dasari, S., Manske, M. K., Abeykoon, J. A., Sarangi, V., Kapoor, P., Paulus, A., Reeder, C. B., Ailawadhi, S., Chanan-Khan, A. A., Kyle, R. A., Gertz, M. A., … Ansell, S. M. (2023). Molecular Clusters and Tumor-Immune Drivers of IgM Monoclonal Gammopathies. *Clinical Cancer Research : An Official Journal of the American Association for Cancer Research*, *29*(5), 957–970. https://doi.org/10.1158/1078-0432.CCR-22-2215

Nadeu, F., Royo, R., Massoni-Badosa, R., Playa-Albinyana, H., Garcia-Torre, B., Duran-Ferrer, M., Dawson, K. J., Kulis, M., Diaz-Navarro, A., Villamor, N., Melero, J. L., Chapaprieta, V., Dueso-Barroso, A., Delgado, J., Moia, R., Ruiz-Gil, S., Marchese, D., Giró, A., Verdaguer-Dot, N., … Campo, E. (2022). Detection of early seeding of Richter transformation in chronic lymphocytic leukemia. *Nature Medicine*, *28*(8), 1662–1671. https://doi.org/10.1038/S41591-022-01927-8

Navin, N., Kendall, J., Troge, J., Andrews, P., Rodgers, L., McIndoo, J., Cook, K., Stepansky, A., Levy, D., Esposito, D., Muthuswamy, L., Krasnitz, A., McCombie, W. R., Hicks, J., & Wigler, M. (2011). Tumour evolution inferred by single-cell sequencing. *Nature*, *472*(7341), 90–95. https://doi.org/10.1038/nature09807

Ocio, E. M., Hernandez, J. M., Mateo, G., Sanchez, M. L., Gonzalez, B., Vidriales, B., Gutierrez, N. C., Orfao, A., & San Miguel, J. F. (2005). Immunophenotypic and cytogenetic comparison of Waldenstrom's macroglobulinemia with splenic marginal zone lymphoma. *Clinical Lymphoma*, *5*(4), 241–245. http://www.ncbi.nlm.nih.gov/pubmed/15794856

Owen, R. G., Treon, S. P., Al-Katib, A., Fonseca, R., Greipp, P. R., McMaster, M. L., Morra, E., Pangalis, G. A., San Miguel, J. F., Branagan, A. R., & Dimopoulos, M. A. (2003). Clinicopathological definition of Waldenström's macroglobulinemia: consensus panel recommendations from the Second International Workshop on Waldenstrom's Macroglobulinemia. *Seminars in Oncology*, *30*(2), 110–115. https://doi.org/10.1053/sonc.2003.50082

Oza, A., & Rajkumar, S. (2015). Waldenström macroglobulinemia: prognosis and management. *Blood Cancer Journal*, *5*(3), e296. https://doi.org/10.1038/bcj.2015.28

Paiva, B., Corchete, L. A., Vidriales, M.-B., Garcia-Sanz, R., Perez, J. J., Aires-Mejia, I., Sanchez, M.-L., Barcena, P., Alignani, D., Jimenez, C., Sarasquete, M.-E., Mateos, M.-V., Ocio, E. M., Puig, N., Escalante, F., Hernandez, J., Cuello, R., Garcia de Coca, A., Sierra, M., … San Miguel, J. F. (2015). The cellular origin and malignant transformation of Waldenstrom macroglobulinemia. *Blood*, *125*(15), 2370–2380. https://doi.org/10.1182/blood-2014-09-602565

Paiva, B., Montes, M. C., García-Sanz, R., Ocio, E. M., Alonso, J., de las Heras, N., Escalante, F., Cuello, R., de Coca, A. G., Galende, J., Hernández, J., Sierra, M., Martin, A., Pardal, E., Bárez, A., Alonso, J., Suarez, L., González-López, T. J., Perez, J. J., … San Miguel, J. F. (2014). Multiparameter flow cytometry for the identification of the Waldenström's clone in IgM-MGUS and Waldenström's Macroglobulinemia: new criteria for differential diagnosis and risk stratification. *Leukemia*, *28*(1), 166–173. https://doi.org/10.1038/leu.2013.124

Poulain, S., Roumier, C., Galiègue-Zouitina, S., Daudignon, A., Herbaux, C., Aiijou, R., Lainelle, A., Broucqsault, N., Bertrand, E., Manier, S., Renneville, A., Soenen, V., Tricot, S., Roche-Lestienne, C., Duthilleul, P., Preudhomme, C., Quesnel, B., Morel, P., & Leleu, X. (2013). Genome wide SNP array identified multiple mechanisms of genetic changes in Waldenstrom macroglobulinemia. *American Journal of Hematology*, *88*(11), 948–954. https://doi.org/10.1002/ajh.23545

Puig, N., Ocio, E. M., Jiménez, C., Paiva, B., Miguel, J. F. S., & García-Sanz, R. (2017). Waldenström's Macroglobulinemia Immunophenotype. In *Waldenström's Macroglobulinemia* (pp. 21–34). Springer, Cham. https://doi.org/10.1007/978-3-319-22584-5_2

Robinson, T. M., Bowman, R. L., Persaud, S., Liu, Y., Gao, Q., Zhang, J., Sun, X., Miles, L. A., Cai, S. F., Sciambi, A., Llanso, A., Famulare, C., Goldberg, A., Dogan, A., Roshal, M., Levine, R. L., & Xiao, W. (2022). Single cell genotypic and phenotypic analysis of measurable residual disease in acute myeloid leukemia. *BioRvix*, 1–15. https://doi.org/10.1101/2022.09.20.508786

Roccaro, A. M., Sacco, A., Jimenez, C., Maiso, P., Moschetta, M., Mishima, Y., Aljawai, Y., Sahin, I., Kuhne, M., Cardarelli, P., Cohen, L., San Miguel, J. F., Garcia-Sanz, R., & Ghobrial, I. M. (2014). C1013G/CXCR4 acts as a driver mutation of tumor progression and modulator of drug resistance in lymphoplasmacytic lymphoma. *Blood*, *123*(26), 4120–4131. https://doi.org/10.1182/blood-2014-03-564583

Rocco, J. W. (2015). Mutant Allele Tumor Heterogeneity (MATH) and Head and Neck Squamous Cell Carcinoma. *Head and Neck Pathology*, *9*(1), 1–5. https://doi.org/10.1007/s12105-015-0617-1

Rodriguez, S., Celay, J., Goicoechea, I., Jimenez, C., Botta, C., Garcia-Barchino, M.-J., Garces, J.-J., Larrayoz, M., Santos, S., Alignani, D., Vilas-Zornoza, A., Perez, C., Garate, S., Sarvide, S., Lopez, A., Reinhardt, H.-C., Carrasco, Y. R., Sanchez-Garcia, I., Larrayoz, M.-J., … Paiva, B. (2022). Preneoplastic somatic mutations including MYD88L265P in lymphoplasmacytic lymphoma. *Science Advances*, *8*(3), eabl4644. https://doi.org/10.1126/SCIADV.ABL4644

Schop, R. F. J., Kuehl, W. M., Van Wier, S. A., Ahmann, G. J., Price-Troska, T., Bailey, R. J., Jalal, S. M., Qi, Y., Kyle, R. A., Greipp, P. R., & Fonseca, R. (2002). Waldenström macroglobulinemia neoplastic cells lack immunoglobulin heavy chain locus translocations but have frequent 6q deletions. *Blood*, *100*(8), 2996–3001. https://doi.org/10.1182/blood.V100.8.2996

Sewastianik, T., Guerrera, M. L., Adler, K., Dennis, P. S., Wright, K., Shanmugam, V., Huang, Y., Tanton, H., Jiang, M., Kofides, A., Demos, M. G., Dalgarno, A., Patel, N. A., Nag, A., Pinkus, G. S., Yang, G., Hunter, Z. R., Jarolim, P., Munshi, N. C., … Carrasco, R. D. (2019). Human MYD88L265P is insufficient by itself to drive neoplastic transformation in mature mouse B cells. *Blood Advances*, *3*(21), 3360–3374. https://doi.org/10.1182/bloodadvances.2019000588

Siegmund, K. D., Marjoram, P., Woo, Y. J., Tavaré, S., & Shibata, D. (2009). Inferring clonal expansion and cancer stem cell dynamics from DNA methylation patterns in colorectal cancers. *Proceedings of the National Academy of Sciences of the United States of America*, *106*(12), 4828–4833. https://doi.org/10.1073/pnas.0810276106

Stone, M. J., & Pascual, V. (2010). Pathophysiology of Waldenström's macroglobulinemia. *Haematologica*, *95*(3), 359–364. https://doi.org/10.3324/haematol.2009.017251

Sun, H., Fang, T., Wang, T., Yu, Z., Gong, L., Wei, X., Wang, H., He, Y., Liu, L., Yan, Y., Sui, W., Xu, Y., Yi, S., Qiu, L., & Hao, M. (2022). Single-cell profiles reveal tumor cell heterogeneity and immunosuppressive microenvironment in Waldenström macroglobulinemia. *Journal of Translational Medicine*, *20*(1), 576. https://pubmed.ncbi.nlm.nih.gov/36494694/

Swerdlow, S. H., Campo, E., Pileri, S. A., Harris, N. L., Stein, H., Siebert, R., Advani, R., Ghielmini, M., Salles, G. A., Zelenetz, A. D., & Jaffe, E. S. (2016). The 2016 revision of the World Health Organization classification of lymphoid neoplasms. *Blood*, *127*(20), 2375–2390. https://doi.org/10.1182/blood-2016-01-643569

Tam, C. S., Opat, S., D'Sa, S., Jurczak, W., Lee, H. P., Cull, G., Owen, R. G., Marlton, P., Ewahlin, B., Sanz, R. G., McCarthy, H., Mulligan, S., Tedeschi, A., Castillo, J. J., Czyz, J., De Larrea, C. F., Belada, D., Libby, E., Matous, J. V., … Huang, J. (2020). A randomized phase 3 trial of zanubrutinib vs ibrutinib in symptomatic Waldenström macroglobulinemia: The ASPEN study. *Blood*, *136*(18), 2038–2050. https://doi.org/10.1182/BLOOD.2020006844

Treon, S. P., Tripsas, C. K., Meid, K., Warren, D., Varma, G., Green, R., Argyropoulos, K. V., Yang, G., Cao, Y., Xu, L., Patterson, C. J., Rodig, S., Zehnder, J. L., Aster, J. C., Harris, N. L., Kanan, S., Ghobrial, I., Castillo, J. J., Laubach, J. P., … Advani, R. H. (2015). Ibrutinib in Previously Treated Waldenström's Macroglobulinemia. *New England Journal of Medicine*, *372*(15), 1430–1440. https://doi.org/10.1056/NEJMoa1501548

Treon, S. P., Tsakmaklis, N., Meid, K., Yang, G., Chen, J. G., Liu, X., Chen, J., Demos, M., Patterson, C. J., Dubeau, T., Gustine, J., Castillo, J. J., Advani, R. H., Palomba, M. L., Xu, L., & Hunter, Z. (2016). Mutated MYD88 Zygosity and CXCR4 Mutation Status Are Important Determinants of Ibrutinib Response and Progression Free Survival in Waldenström's Macroglobulinemia. *Blood*, *128*(22), 2984. http://www.bloodjournal.org/content/128/22/2984?sso-checked=true

Treon, S. P., Xu, L., Yang, G., Zhou, Y., Liu, X., Cao, Y., Sheehy, P., Manning, R. J., Patterson, C. J., Tripsas, C., Arcaini, L., Pinkus, G. S., Rodig, S. J., Sohani, A. R., Harris, N. L., Laramie, J. M., Skifter, D. a, Lincoln, S. E., & Hunter, Z. R. (2012). MYD88 L265P somatic mutation in Waldenström's macroglobulinemia. *The New England Journal of Medicine*, *367*(9), 826–833. https://doi.org/10.1056/NEJMoa1200710

Varettoni, M., Zibellini, S., Defrancesco, I., Ferretti, V. V., Rizzo, E., Malcovati, L., Gallì, A., Giovanni, M., Porta, D., Boveri, E., Arcaini, L., Candido, C., Paulli, M., & Cazzola, M. (2017). Pattern of somatic mutations in patients with Waldenström macroglobulinemia or IgM monoclonal gammopathy of undetermined significance. *Haematologica*, *102*(12), 2077–2085. https://doi.org/10.3324/haematol.2017.172718

Wang, E., Mi, X., Thompson, M. C., Montoya, S., Notti, R. Q., Afaghani, J., Durham, B. H., Penson, A., Witkowski, M. T., Lu, S. X., Bourcier, J., Hogg, S. J., Erickson, C., Cui, D., Cho, H., Singer, M., Totiger, T. M., Chaudhry, S., Geyer, M., … Abdel-Wahab, O. (2022). Mechanisms of Resistance to Noncovalent Bruton's Tyrosine Kinase Inhibitors. *New England Journal of Medicine*, *386*(8), 735–743. https://doi.org/10.1056/nejmoa2114110

Xu, L., Tsakmaklis, N., Yang, G., Chen, J. G., Liu, X., Demos, M., Kofides, A., Patterson, C. J., Meid, K., Gustine, J., Dubeau, T., Palomba, M. L., Advani, R., Castillo, J. J., Furman, R. R., Hunter, Z. R., & Treon, S. P. (2017). Acquired mutations associated with ibrutinib resistance in Waldenstrom Macroglobulinemia. *Blood*, *129*(18), 2519–2525. https://doi.org/10.1182/blood-2017-01-761726

Yates, L. R., Gerstung, M., Knappskog, S., Desmedt, C., Gundem, G., Van Loo, P., Aas, T., Alexandrov, L. B., Larsimont, D., Davies, H., Li, Y., Ju, Y. S., Ramakrishna, M., Haugland, H. K., Lilleng, P. K., Nik-Zainal, S., McLaren, S., Butler, A., Martin, S., … Campbell, P. J. (2015). Subclonal diversification of primary breast cancer revealed by multiregion sequencing. *Nature Medicine*, *21*(7), 751–759. https://doi.org/10.1038/nm.3886

Figures and Table

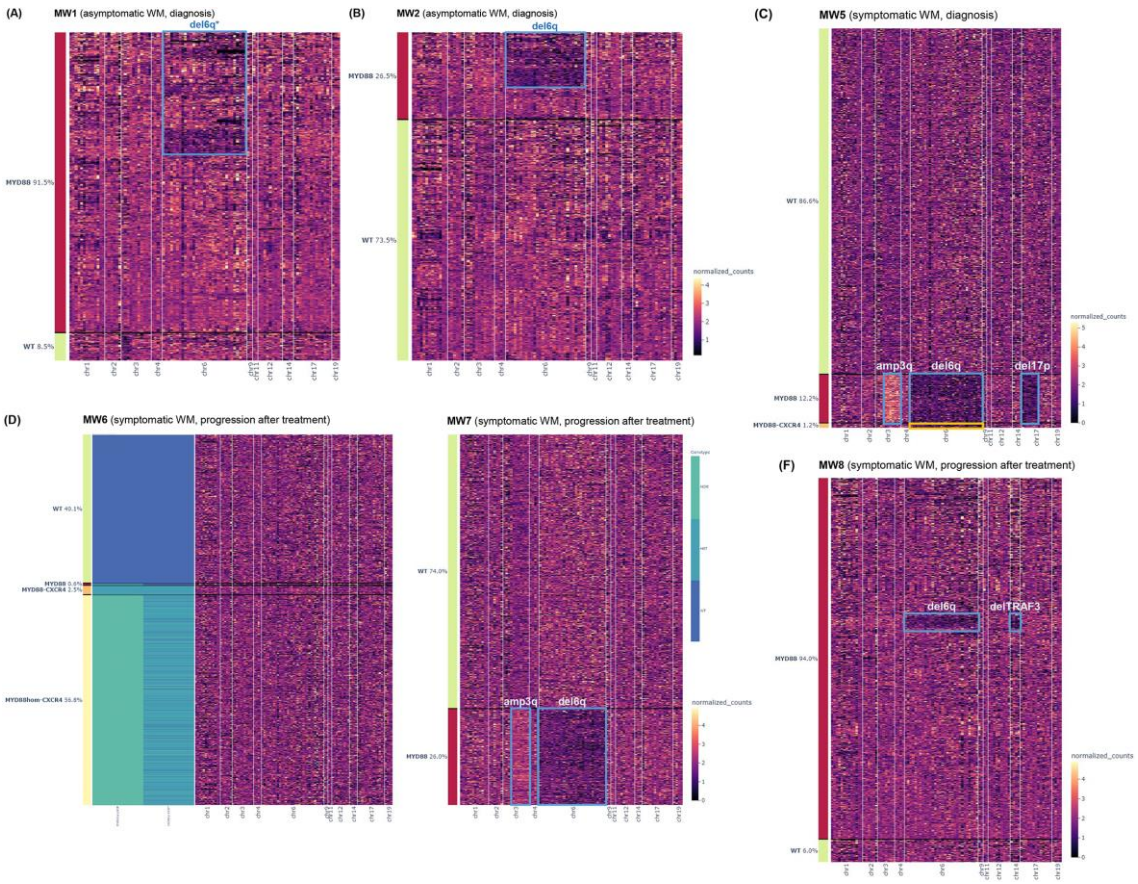

Fig 1. Clonal architecture of different disease stages of Waldenström's macroglobulinemia at the single-cell level.

(A) Presence of wild-type (green) versus heterozygous *MYD88*^{L265P} (red) and deletion of 6q (blue) in an asymptomatic Waldenström's macroglobulinemia patient at diagnosis (MW1). Rows represent the individual cells and columns represent the regions covered by the panel amplicons. Color scale indicates the number of normalized reads for copy number alterations. **(B)** Presence of wild-type (green) versus heterozygous *MYD88*^{L265P} (red) and deletion of 6q (blue) in an asymptomatic Waldenström's macroglobulinemia patient at diagnosis (MW2). Rows represent the individual cells and columns represent the regions covered by the panel amplicons. Color scale indicates the number of normalized reads for copy number alterations.

(C) Distribution of somatic variants (*MYD88*^{L265P} and *CXCR4*^{S344*}) and copy number alterations (deletion of 6q, deletion of 17p and amplification of 3q) in a patient with symptomatic Waldenström's macroglobulinemia at diagnosis (MW5). Rows represent

the individual cells and columns represent the regions covered by the panel amplicons. Color scale indicates the number of normalized reads for copy number alterations.

(D) Distribution of somatic variants (*MYD88*^{L265P}, heterozygous and homozygous, and *CXCR4*^{S338*}) in one symptomatic Waldenström's macroglobulinemia patient at disease progression (MW6). Rows represent the individual cells and columns represent the regions covered by the panel amplicons. Color scale indicates the number of normalized reads for copy number alterations. **(E)** Distribution of somatic variants (heterozygous *MYD88*^{L265P}) and copy number alterations (deletion of 6q and amplification of 3q) in one symptomatic Waldenström's macroglobulinemia patient at disease progression (MW7). Rows represent the individual cells and columns represent the regions covered by the panel amplicons. Color scale indicates the number of normalized reads for copy number alterations.

(F) Presence of *MYD88*^{L265P}, deletion of 6q and deletion of *TRAF3* in one patient with symptomatic Waldenström's macroglobulinemia at the time of disease progression. Rows represent the individual cells and columns represent the regions covered by the panel amplicons. Color scale indicates the number of normalized reads for copy number alterations.

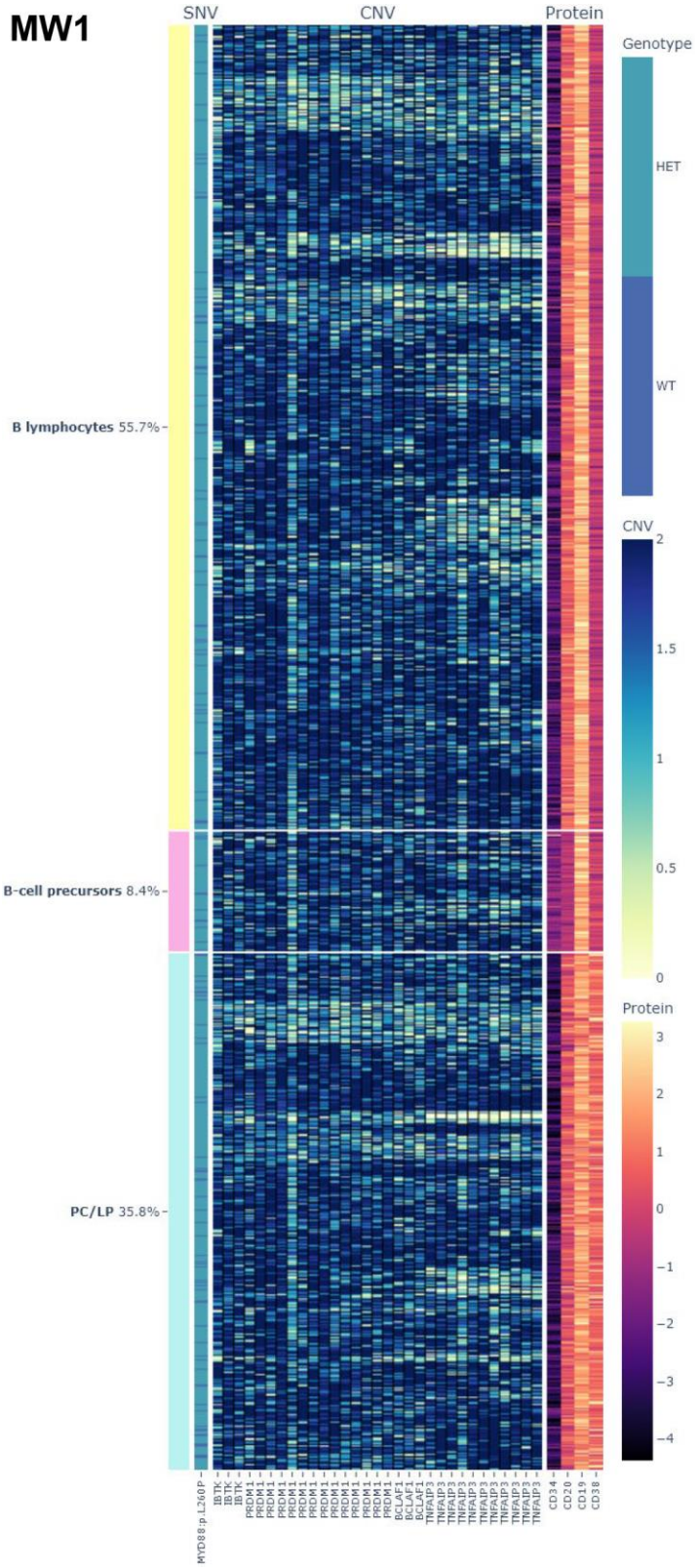

Fig. 2. Copy number alterations in selected regulatory regions of 6q in one patient with asymptomatic Waldenström's macroglobulinemia. Rows represent the individual cells and columns represent the amplicons of 6q region. Yellow-blue color scale indicates the copy number alterations. The number of deleted amplicons/genes differed between cells, being TNFAIP3 the most frequently deleted gene.

Table 1. Patients' characteristics.

ID	Time-point	Year	Disease	Treatment	Del6q by FISH	Immunophenotype
MW1 CD19+	**Diagnosis**	**2021**	**asymptomatic WM**	**-**	**-**	10.1% B-cells: CD19+CD20+CD38- 0.2% PC/LP: CD19+CD20-/+(71%)CD38+IgM+CD56-CD5-CyK+CD81+CD117-CD79b-/+(71%)CD27+CD45+ 1.5% normal B-cells
MW2	**Diagnosis**	**2021**	**asymptomatic WM**	**-**	**39%**	6.2% B-cells: CD19+CD20+CD38+ 0.5% LP: CD19+CD20+CD38+CD22-CD25-CyK+CD45+IgM+ 0.5% normal B-cells
MW3 CD19+	**Diagnosis**	**2021**	**symptomatic WM**	**-**	**-**	2.3% B-cells: CD19+w CD20+CD38- 0.2% PC/LP: CD19+CD20-/+w(35%)CD38+CD138+w IgM+ 1.4% normal B-cells
MW4 CD19+	**Diagnosis**	**2021**	**symptomatic WM**	**-**	**no**	10.5% B-cells: CD19+w CD20+CD38- 0.6% PC: CD19+CD20-/+w CD38+IgM++CD56-CD5-CyK+CD81+CD117-CD79b+w CD27+CD45+ 1% normal B-cells
MW5	Diagnosis **Diagnosis**	2017 **2021**	IgM-MGUS **symptomatic WM**	- BTKi (1st line)	- **-**	10.6% B-cells: CD19+CD20+CD38- 1% LP: CD20+CD38+w IgM+CD56-CyK+CD27-/+w HLADR+CD79b+CD45+ 0.3% normal PC 0.2% normal B-cells
MW6	Diagnosis Progression **Progression**	2014 2015 **2021**	symptomatic WM	DRC (1st line): PR bendamustine and rituximab (2nd line): PR ibrutinib (3rd line): PR	no no **no**	25.4% B-cells: CD19+CD20+w CD38-CD22+w CD25+Cyλ+CD45+ 1% PC: CD19+CD38++CyK+ 0.2% normal B-cells
MW7	Diagnosis Diagnosis Progression	2001 2008 2011 **2021** 2022	IgM-MGUS symptomatic WM	- - DRC (1st line): PR ibrutinib (2nd line): SD rituximab (3rd line): PR	- 29% - **-** -	13% B-cells: CD19+CD20+CD38+w CD10-CD45+CyK+Cyλ- 0.01% PC 0.04% normal B-cells
MW8 CD19+	Diagnosis	2014	asymptomatic WM	-	no	

Diagnosis	2015	symptomatic WM	BDR (1st line): SD	-	
Progression	2016		ibrutinib (2nd line): PR	no	
Progression	**2021**		anti-MALT1 (3rd line)	**25%**	25% B-cells: CD19+CD20+CD38-/+w IgM+w Cyλ+CD45+ 2.1% LP: CD19+CD20+CD38+w CyL+CD45+ 0.04% normal PC 1.1% normal B-cells
Progression	2022		anti-BCL2 (4th line): SD	16%	
Progression	2022		BTKi (5th line)	11%	

BCL2, B-cell CLL/Lymphoma 2; BDR, bortezomib, dexamethasone and rituximab; BTKi, Bruton's tyrosine kinase inhibitor; Cy, intracytoplasmic; del6q, deletion of chromosome 6q; DRC, dexamethasone, rituximab and cyclophosphamide; FISH, fluorescence in situ hybridization; IgM, immunoglobulin M; LP, lymphoplasmacytes; MALT1, mucosa-associated lymphoid tissue lymphoma translocation protein 1; MGUS, monoclonal gammopathy of uncertain significance; PC, plasma cells; PR, partial response; SD, stable disease; w, weak; WM, Waldenström's macroglobulinemia

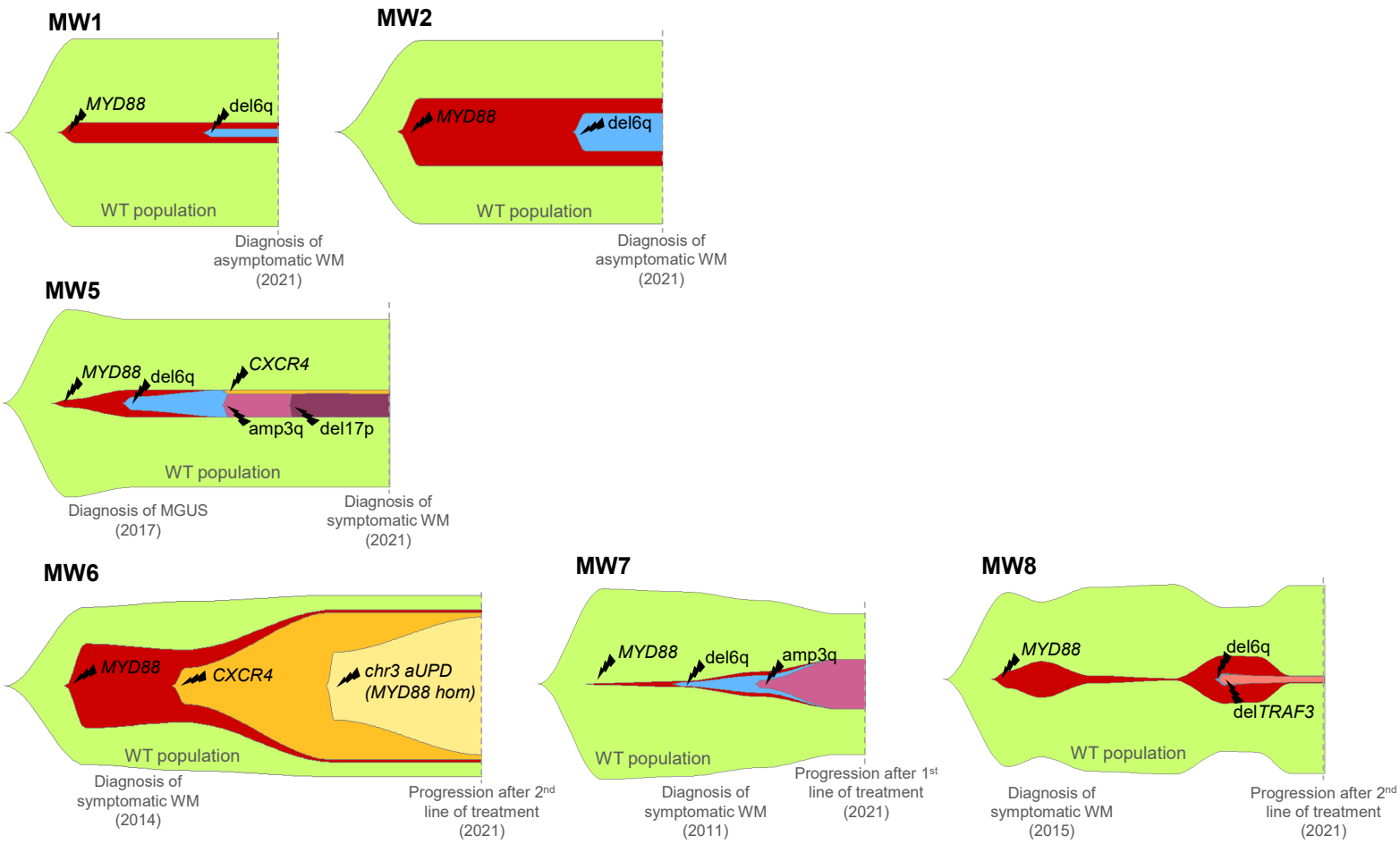

Amp3q, amplification of chromosome 3q; chr3 aUPD, acquired uniparental disomy of chr3; del17p, deletion of chromosome 17p; del6q, deletion of chromosome 6q; del*TRAF3*, deletion of *TRAF3* gene (chromosome 14); hom, homozygous for *MYD88*^{L265P}; WM, Waldenström's macroglobulinemia; WT, wild-type

Fig. S1. Fishplots representing the hypothesized evolution of the clones in eight Waldenström's macroglobulinemia patients. The proposed order of the events was inferred based on single-cell data, FISH results, and the patients' clinical history.

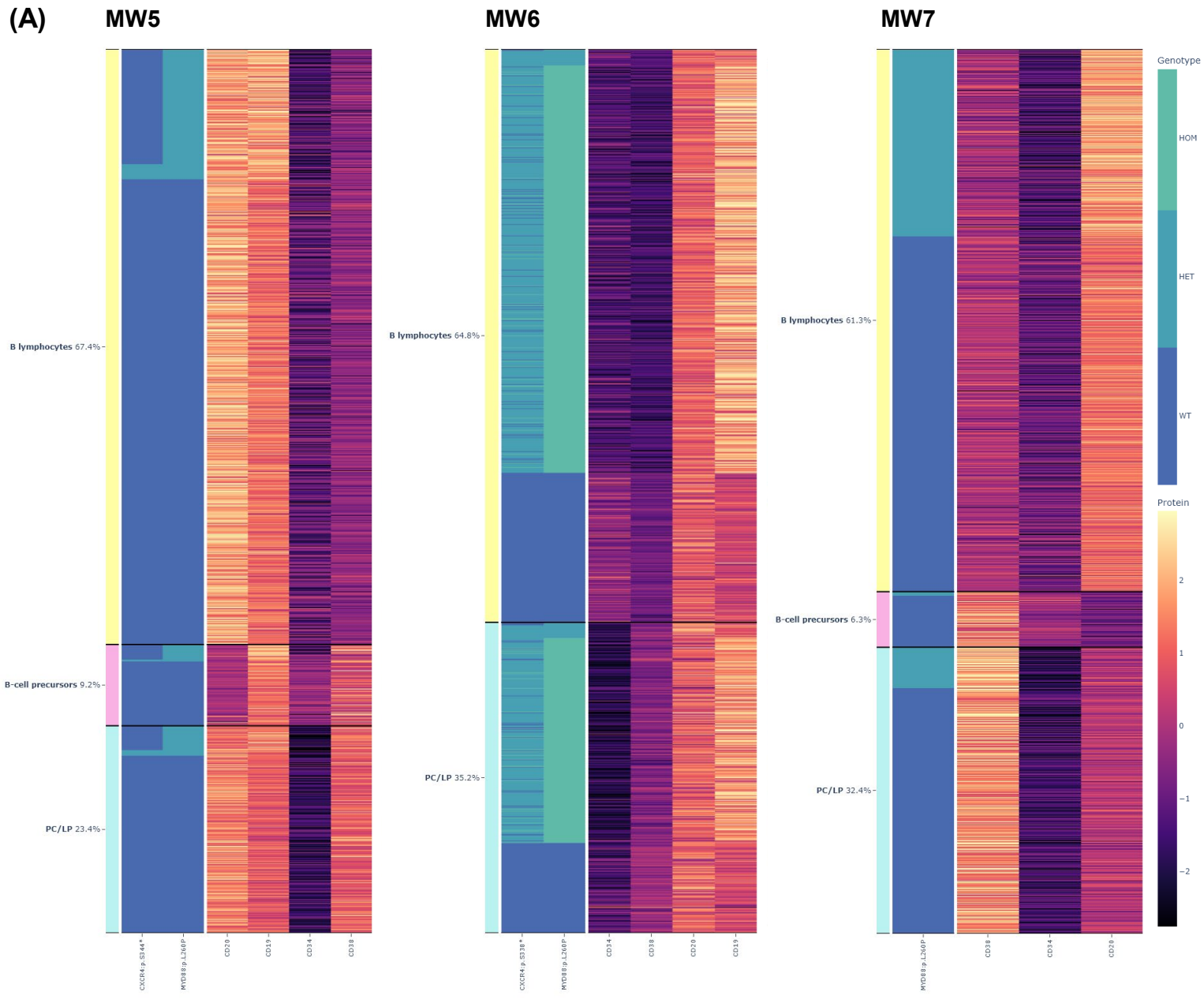

Het, heterozygous; Hom, homozygous; PC/LP, plasma cells/plasmacytoid lymphocytes; WT, wild-type

Fig. S2. Combined representation of genotype and phenotype of Waldenström's macroglobulinemia single cells.

(A) Genotype and phenotype of the cell populations in three Waldenström's macroglobulinemia patients. Cells were clustered based on the expression of CD19, CD20, CD34 and CD38 antigens and designated as the different cell populations (B lymphocytes, B-cell precursors, and plasma cells). Status of the somatic variants (*MYD88* and *CXCR4*) within each population is represented in green and blues. Rows represent the individual cells and columns represent the somatic mutations and the antigen expression. Color scale indicates the intensity of antigen expression.

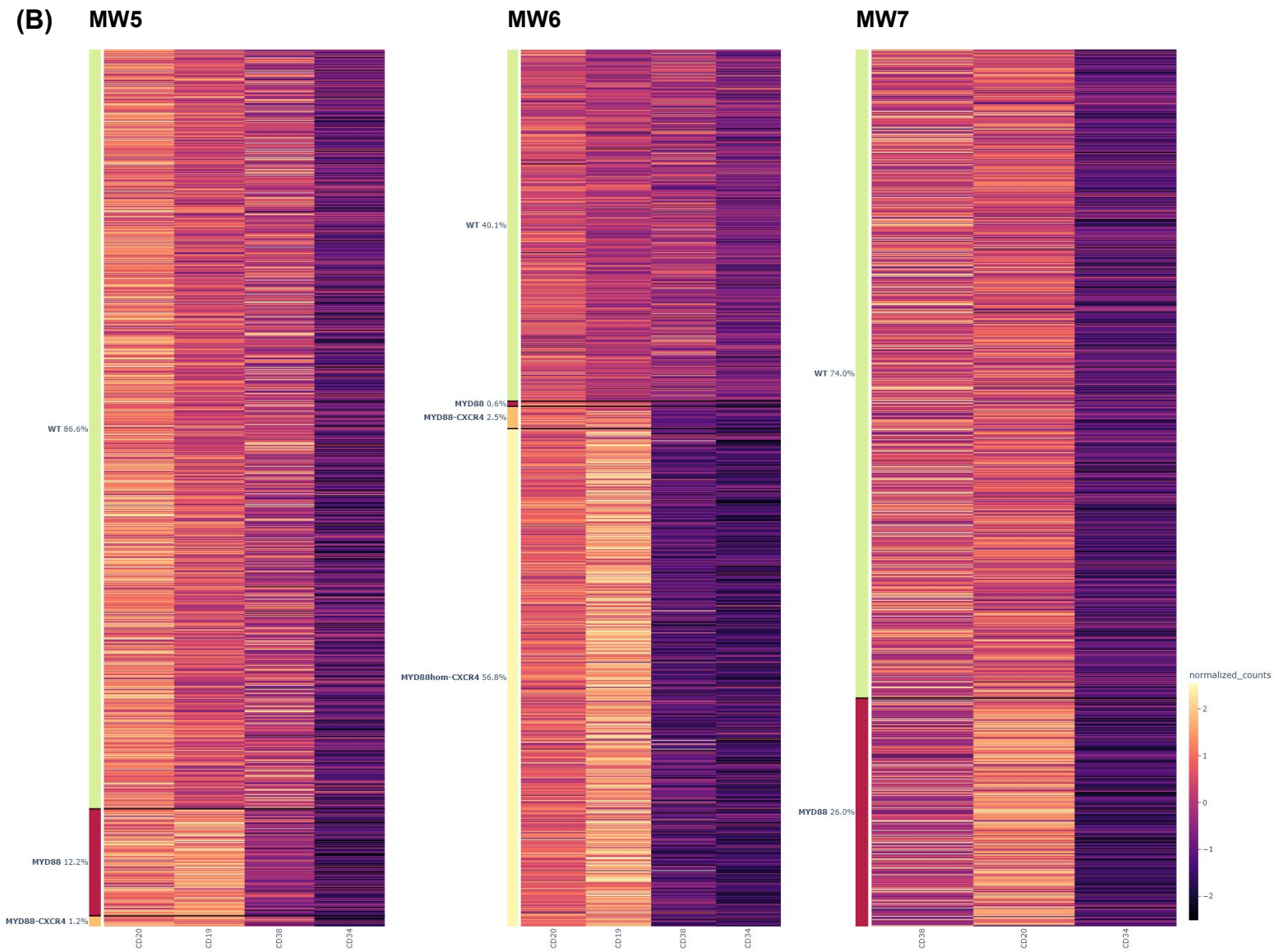

Hom, homozygous; WT, wild-type

(B) Antigen expression in the single cells clustered by genotype of three Waldenström's macroglobulinemia patients. Expression of CD19, CD20, CD34, and CD38 is different in (*MYD88* and *CXCR4*) mutated cells compared to wild-type cells. Rows represent the individual cells and columns represent the antigen expression. Color scale indicates the intensity of antigen expression.

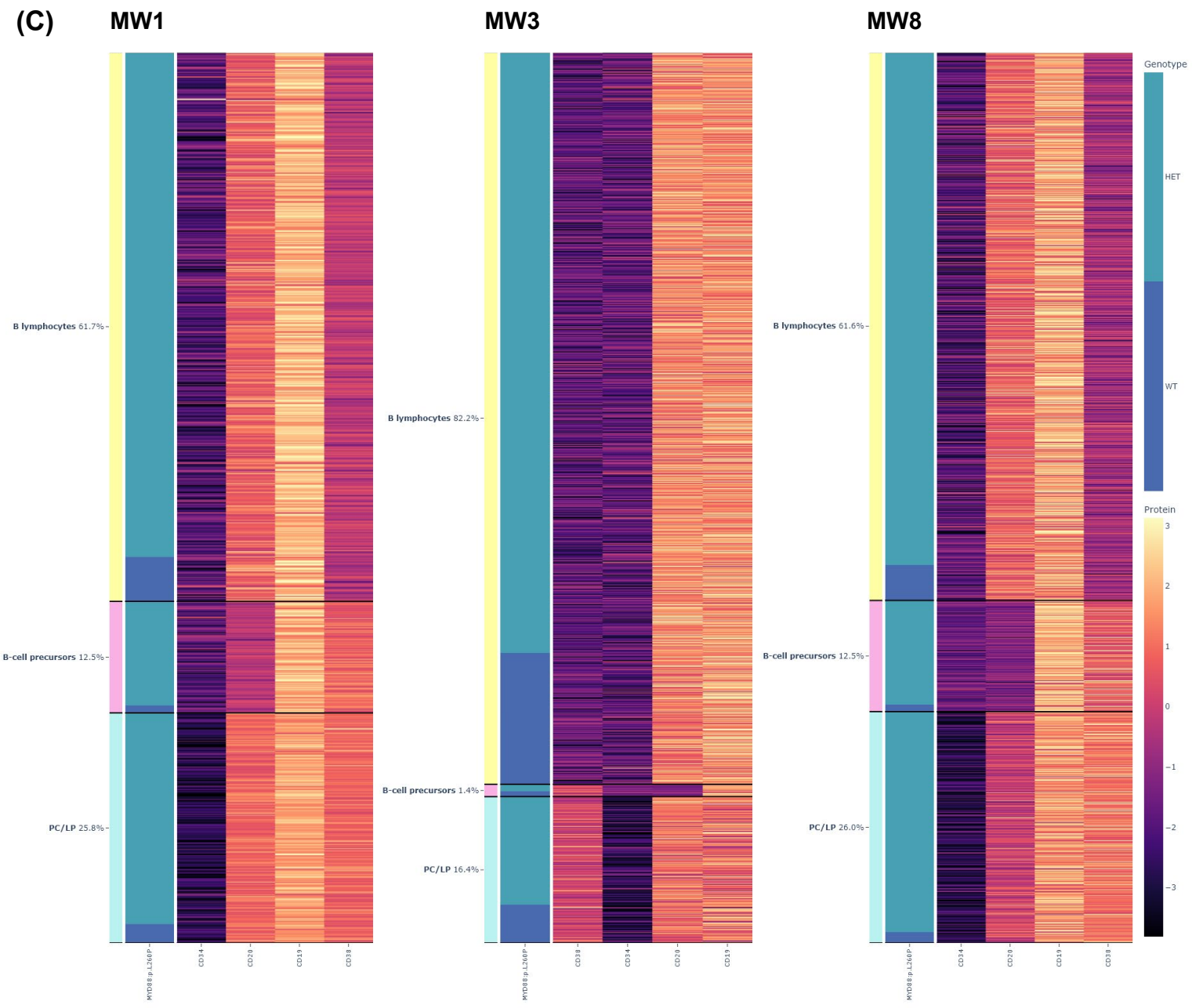

Het, heterozygous; PC/LP, plasma cells/plasmacytoid lymphocytes; WT, wild-type

(C) Genotype and phenotype of the cell populations in three Waldenström's macroglobulinemia patients. Cells were clustered based on the expression of CD19, CD20, CD34 and CD38 antigens and designated as the different cell populations. Status of the somatic variant (*MYD88*^{L265P}) within each population is represented in green and blue. Rows represent the individual cells and columns represent the somatic mutations and the antigen expression. Color scale indicates the intensity of antigen expression. As these were CD19 negative depleted samples, most cells were *MYD88*-mutated, and no differences in the antigen expression could be observed based on the genotype.

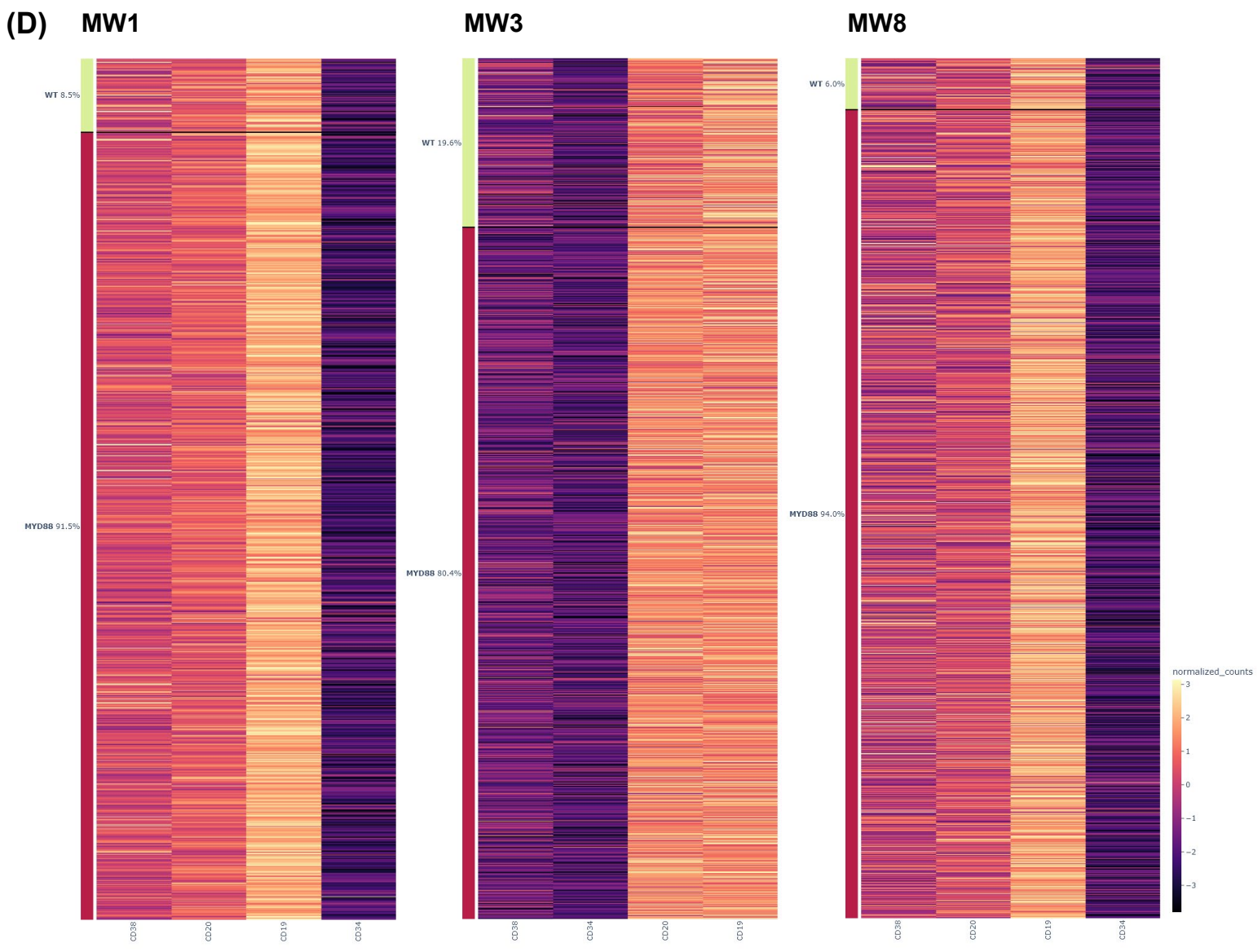

WT, wild-type

(D) Antigen expression in the single cells clustered by genotype of three Waldenström's macroglobulinemia patients. As these were CD19 negative depleted samples, most cells were *MYD88*-mutated, and no differences in the antigen expression could be observed in mutated cells compared to wild-type cells. Rows represent the individual cells and columns represent the antigen expression. Color scale indicates the intensity of antigen expression.